NASA Contractor Report 145361

SIDE-FORCE ALLEVIATION ON SLENDER, POINTED FOREBODIES
AT HIGH ANGLES OF ATTACK

(NASA-CR-145361) SIDE-FORCE ALLEVIATION ON SLENDER, POINTED FOREBODIES AT HIGH ANGLES OF ATTACK (Old Dominion Univ., Norfolk, Va.) 25 p HC A02/MF A01 CSCL 01A

N78-25053

Unclas
G3/02 21558

Dhanvada M, Rao

OLD DOMINION RESEARCH FOUNDATION
Norfolk, VA 23508

NASA Grant NSG-1315
May 1978

National Aeronautics and
Space Administration

Langley Research Center
Hampton, Virginia 23665

SIDE-FORCE ALLEVIATION ON SLENDER, POINTED FOREBODIES AT HIGH ANGLES OF ATTACK

by Dhanvada M. Rao

Research Associate, Old Dominion University Research Foundation, Norfolk, Virginia

Abstract

A new device* has been proposed for alleviating high angle-of-attack side force on slender, pointed forebodies. A symmetrical pair of separation trips in the form of helical ridges are applied to the forebody to disrupt the primary lee-side vortices and thereby avoid the instability that produces vortex asymmetry. Preliminary wind tunnel tests at Mach 0.3 and Reynolds no. 5.25×10^6 on a variety of forebody configurations and on a wing-body combination at angles of attack up to 56 degrees, demonstrated the effectiveness of the device.

---

*Patent applied for.

Research supported by NASA under Grant no. NSG 1315.

SIDE-FORCE ALLEVIATION ON SLENDER, POINTED FOREBODIES
AT HIGH ANGLES OF ATTACK

1. Introduction

The emphasis on combat agility in the new generation of fighter aircraft calls for controlled flight capability to increasingly high angles of attack. The pointed, slender forebody shapes commonly employed on such aircraft characterstically experience abrupt and relatively large out-of-plane aerodynamic loads when pitched to high angles. Accompanied by deteriorating control effectiveness at high angles of attack, serious handling difficulties in rapid maneuvering are encountered. The prevention of side force or its alleviation is an important current technology need.

It is well established* that the origin of the out-of-plane loads lies in an asymmetric development of the leeward vortex wake of slender, pointed-nose lifting bodies. In the research so far, the two-dimensional impulsive flow analogy has served as a useful framework for analytical prediction of the oscillatory side force due to alternate vortex shedding along the body length with increasing angle of attack. There is mounting experimental evidence, however, that the onset and initial build-up of the asymmetric loading is determined by flow development close to the apex. Lack of detailed knowledge of the fluid-dynamics of apex vortices viz. their growth and stability, impedes the search for aerodynamic means of side-force suppression.

---

*See reference 1 for a recent summary of the subject and pertinent references.

From a practical viewpoint, any solution proposed for the high angle-of-attack side force problem must not compromise the vehicle performance in normal flight (e.g. cruise drag, stability etc.). Any modification of or installation in the nose region is conditional to compatibility with the radome electronic requirements. A passive device is preferred, and one that would lend itself to retro-fitting without significant structural or other modifications to in-service aircraft.

Although many devices have been proposed and wind-tunnel tested, no universally acceptable method for side-force alleviation meeting all the above criteria has emerged so far. Notable among successful aerodynamic devices are the nose strakes[1]. However, strakes introduce undesirable physical discontinuities in the radome and also generate persistent trailing vortices even at lower angles of attack which can adversely interact with downstream aerodynamic components such as canards, air-intakes, wing leading-edge devices and tail surfaces. Keeping in view such practical constraints, an alternative approach towards side-force alleviation has been proposed.

2. A New Approach

The present approach is to modify in a basic manner the normal fluid-dynamic process which generates the familiar contra-rotating pair of lee-side vortices from forebody cross-flow separation. These primary vortices represent concentrations of vorticity shed uniformly along a meridional separation line on either side of the body, and their influence dominates the lee-surface pressures. The twin vortices are symmetrically disposed initially, but on reaching a critical angle of attack they begin to grow asymmetrically. The resulting skewness in the perpheral pressure distribution then generates a side-force component.

Side-force suppression could be achieved by artificially stabilizing the primary vortices or by preventing their formation. The latter option was pursued and, recalling the experience of periodic-wake suppression on circular cylinders in two-dimensional flow[2], it was reasoned that these lee-side vorticity concentrations might be disrupted by imposing sufficient non-uniformity in the vorticity flux along the separation lines. Accordingly, a separation trip was devised in the form of a symmetrical pair of surface ridges, starting at the top near the apex, following a helical path around the sides and terminating near the bottom rear of the forebody. This trajectory not only passes through varying levels of boundary layer vorticity along the body as desired, but also places the ridge favorably i.e. at an angle approaching 90 degrees to the predominant boundary layer flow direction with increasing angle of attack, for enhanced effectiveness as a separation trip. At normal angles of attack, on the other hand, such a ridge would be presented obliquely to the boundary layer streamlines and thus cause only a minor disturbance.

With the helical ridges described above, it was envisioned that the normal lee-side vortex pair would be replaced by a multiplicity of weaker vortices. Such an ensemble of vortices was considered less likely to develop a coherent asymmetry for significant side force to be generated. Also, a multiple-vortex wake was expected to decay more rapidly and therefore minimize interference effects over the downstream components.

3. Wind Tunnel Tests

Proof-of-concept tests were carried out in the NASA-Langley 7 x 10 ft. wind tunnel at low subsonic speed. The experimental program was in three parts, according to the objectives and type of model used, as follows:

I. Preliminary investigation on a general research fuselage model to evaluate ridge variations, through forebody loads measured directly on a separate balance,

II. Ridge effectiveness test on a fuselage-wing configuration obtained by mounting a 60 deg. swept-back wing to the fuselage of (I), through overall longitudinal and lateral-directional characteristics, and

III. Tests on two pointed axi-symmetric bodies, an ogive-cylinder and a cone-cylinder, in order to include additional forebody shapes tested by other investigators.

The basic geometry and dimensions of the models are presented in figure 1. A photograph of model (II) fitted with the anti-side-force device is shown in figure 2. The ridges were 3.18 or 1.59 mm diameter solder wire attached to the forebody by means of epoxy cement.

The free-stream conditions were maintained nominally constant in all the tests at Mach 0.3 and Reynolds number 0.53×10^6 per meter. The angle of attack ranged from -4° to 48° (models I and II) and 56° (models III) except when excessive model vibration forced the test to be terminated at a lower angle.

Six-component measurements were obtained on models (I) and (II) using a dual balance system which permitted forebody loads to be recorded separately. The balance data were reduced to coefficient form referenced to maximum body cross-section area and length (for models I and III) or wing area, mean aerodynamic chord and span for model II (with the exception of fig. 10 where fuselage data with and without wing are compared).

4. Discussion of Results

I) Fuselage Alone:

The side force onset on the forebody occurred at $\alpha = 30^{o}$ (fig. 3) which is in fair agreement with the correlated data of reference 1 on the basis of nose angle and length/diameter ratio. Comparison with some early data available on the same model showed good repeatability.

With 3.18 mm diameter straight ridges installed along the side meridians of the forebody, no improvement appeared in the side-force characteristics (fig. 4). Similar finding has been reported on models with full-length side strakes in reference 3.

The 3.18 mm diameter helical ridges reduced the forebody side force essentially to zero, within the estimated accuracy of the balance (i.e. $\pm$ 0.5% of maximum side force capacity), over the entire angle of attack range (fig. 5). The degree of side-force suppression was found to be sensitive to asymmetry in the ridge pair; it is believed that the residual side force (inconsequential as it is) was due to a small but noticeable asymmetry of the ridges*.

As an indirect test of the postulated mechanism behind the present device, the model was rolled 180^{o}. This would tend to aline the helical ridge (now running bottom to top) approximately with rather than across the boundary layer flow at high angles of attack, thereby neutralizing its effectiveness as a separation trip. In this test as anticipated the side-force suppression capability of the helical ridge was completely lost (fig. 6).

*The ridge installation was carried out at the tunnel site without the aid of any jigs etc.

Returning the model to its original (0° roll) position, the 3.18 mm helical ridges were truncated as shown in figure 7. This ad-hoc modification was tried mainly to assess the role of the apex formed by the ridge junction. Some degradation in effectiveness appeared around 40° to 45° angle of attack, although the maximum side force recorded remained quite small. A more definitive study of ridge truncation is needed to isolate the most critical portions of the device, particularly in the nose region typically occupied by a radome.

A full-length ridge pair identical in shape to the original helical ridges but of half the diameter (1.59 mm) suppressed the side force up to about $\alpha = 40^\circ$ (fig. 8). From the limited data available from the present test, the optimum ridge height Reynolds number (based on free-stream unit Reynolds number) would appear to lie between 0.1×10^5 and 0.2×10^5 (note that this applies to the circular cross-section ridges tested; other section shapes e.g. those having a sharp corner, may be found to be more effective).

The forebody contribution to directional characteristics at 10^0 sideslip remained essentially unaltered by the addition of 3.18 mm helical ridges, up to 40° angle of attack (fig. 9). Beyond that angle, the ridges appeared to produce a stabilizing trend by reducing the adverse side force and yawing moment, in direct contrast to the "clean" forebody. Additional data, in the form of detailed sideslip traverses at various constant angles of attack, will be needed for a more complete assessment of the directional stability effects of the present device.

II) Fuselage/Wing Combination:

Addition of the wing to the aft-fuselage accentuated the forebody side force development, and almost doubled the maximum side-force amplitude (fig. 10). This reflects the increased normal force carried by the forebody due to upwash ahead of the wing. Comparison of the nose balance and main balance data indicates a significant side load developing over the rear half of the model even before the onset of side force on the forebody. This is attributed to misalinements in the model assembly and/or support system leading to a small effective side-slip of the configuration. (A repeatable bias in the oil-flow visualizations of the zero-sideslip, high angle-of-attack flow patterns obtained during a previous investigation with the same model lends support to this contention).

Even with the relatively magnified side force and yawing moment on this model the efficacy of 3.18 mm helical ridges was fully confirmed (fig. 11). The rolling moment found on the "clean" model above the side-force onset angle of attack (presumably arising from the asymmetric forebody vortices interacting with the wing) was eliminated at the same time.

The longitudinal characteristics of the configuration indicated that the helical ridges produced negligible change in the drag polar as well as in pitch stability up to $\alpha = 28^{\circ}$ (viz. the side-force onset angle), figure 12. Beyond this angle of attack, the erratic lift behaviour of the "clean" model was markedly smoothened and improved.

III) Axi-symmetric Bodies:*

The ogive-cylinder model in "clean" condition produced a steadily increasing side force starting at $\alpha = 35^{\circ}$, but at 52° went into a violent

*These data were furnished by Mr. Charles H. Fox, Jr., of NASA Langley and potentially dangerous sideways oscillation (presumably due to unsteady vortex-shedding induced excitation of the sting-support at its natural frequency), requiring the test to be stopped. With 3.18 mm helical ridges installed over the forebody, the side force was practically eliminated and no unsteadiness encountered up to the maximum available angle of attack (fig. 13A).

The "clean" cone-cylinder model similarly could not be tested above $\alpha = 44^{\circ}$. With 3.18 mm helical ridges affixed to the conical portion, the side force was essentially suppressed and normal testing could proceed to the angle of attack limit (fig. 13B).

5. Conclusions

These preliminary tests, covering a few basic configurations of practical interest, fully confirmed the efficacy of helical ridges in alleviating the high angle-of-attack side force on slender, pointed forebodies. Associated benefits demonstrated on a fighter-type wing-body combination were the elimination of rolling moment accompanying the side-force onset and a smoothening of the erratic post-stall lift behaviour, implying an overall improvement in handling characteristics near maximum lift. Remarkably, the precise trajectory of the helical ridges appeared not to be critical (within limits as yet unknown); in all cases the ridge shape was aribtrarily specified as a smooth curve and success achieved in the very first trial on all models. The helical ridges without question exert a powerful influence on the high angle of attack separated flowfield of slender pointed bodies, and a detailed experimental investigation appears to be in order to fully understand the fluid dynamics involved.

References

1. "Asymmetric aerodynamic forces on aircraft forebodies at high angles of attack" by Gary T. Chapman, AGARD CP-199, Paper no. 12, 1976

2. "The conditions of separation and vortex formation past cylinders" by A. Naumann et al, AGARD CP-4, pp. 547-674, 1966.

3. "Experimental aerodynamic characteristics for a cylindrical body of revolution with side strakes and various noses at angles of attack from 0° to 58° and Mach numbers from 0.6 to 2.0" by Leland H. Jorgensen and Edgar R. Nelson, NASA TM X-3130, 1975.

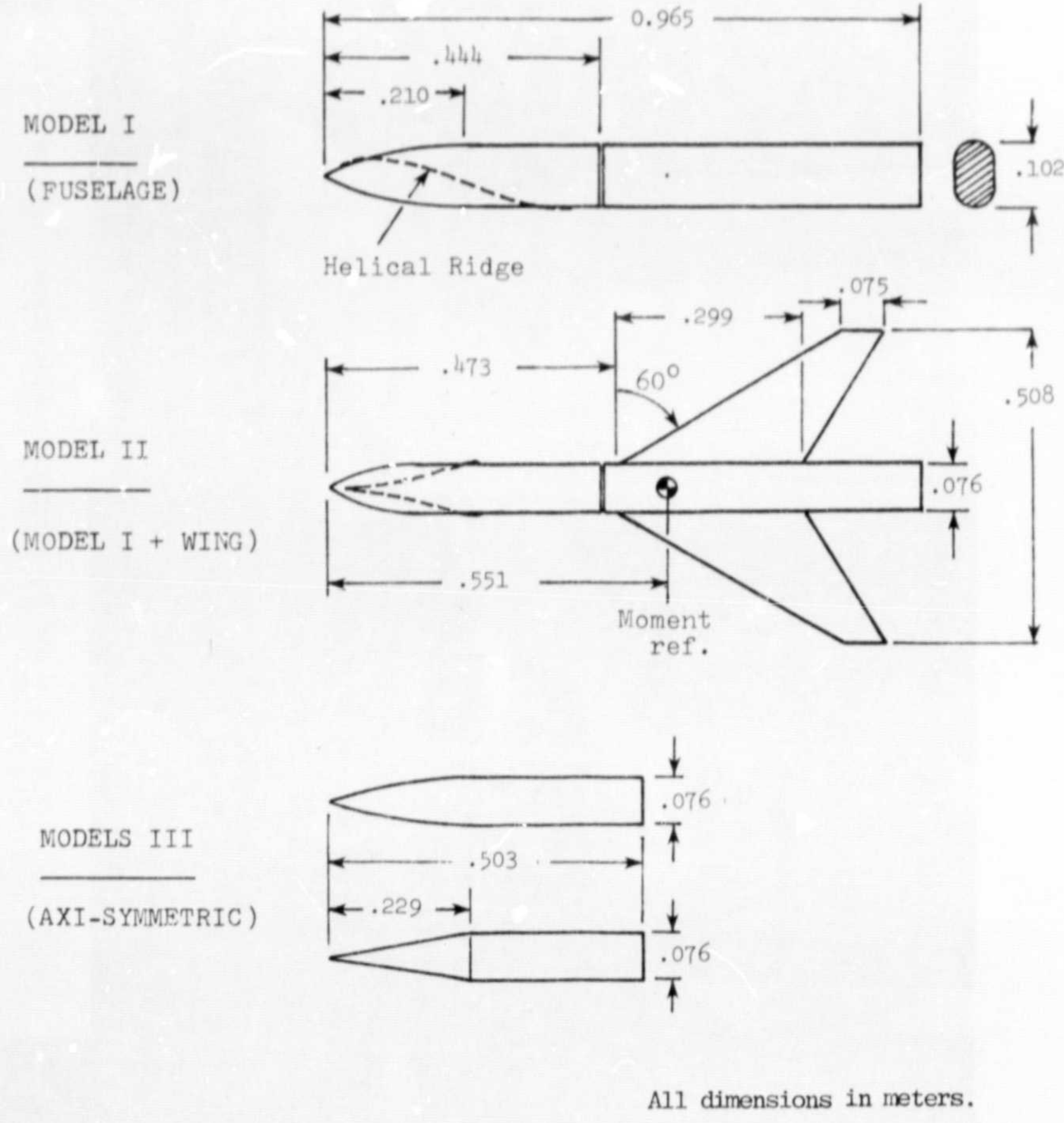

Fig.1 Basic geomtery and dimensions of models

Fig.2 Photograph of Model II mounted in wind-tunnel test section.

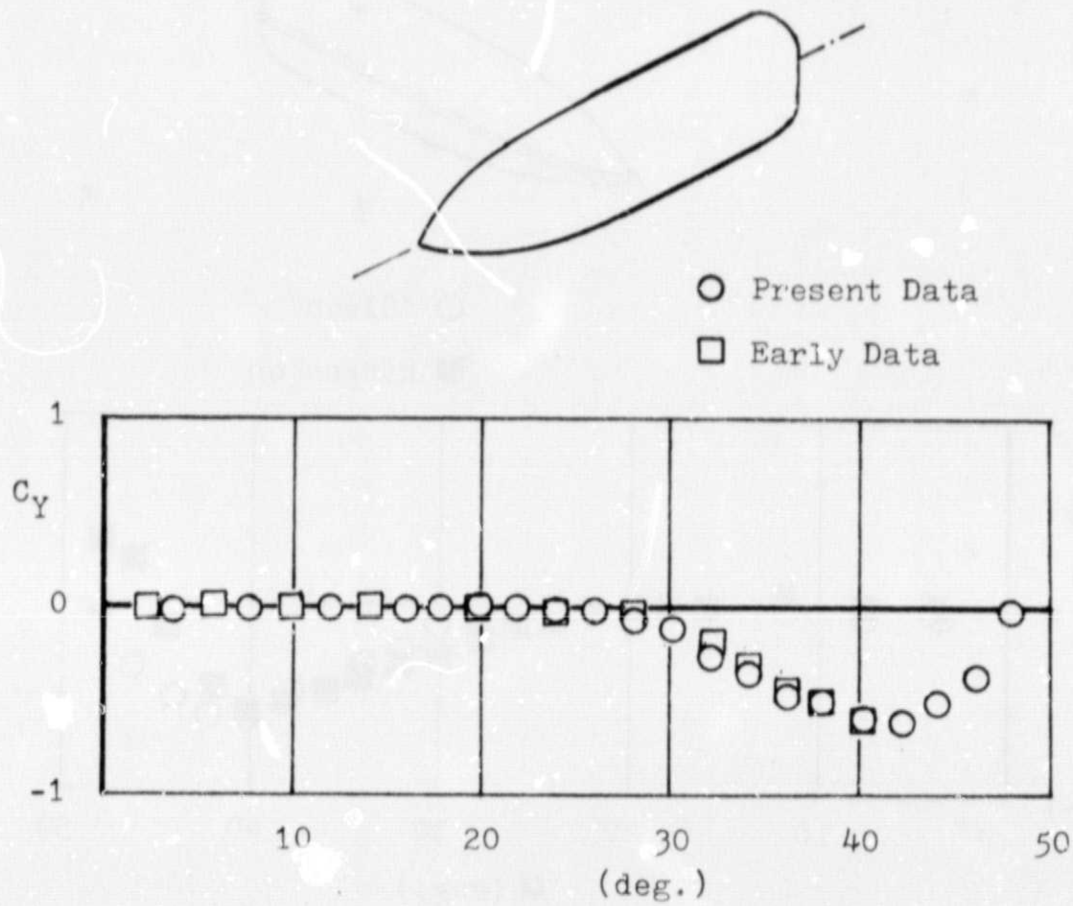

Fig.3 "Clean" forebody (Model I): Side force coeff. versus angle of attack

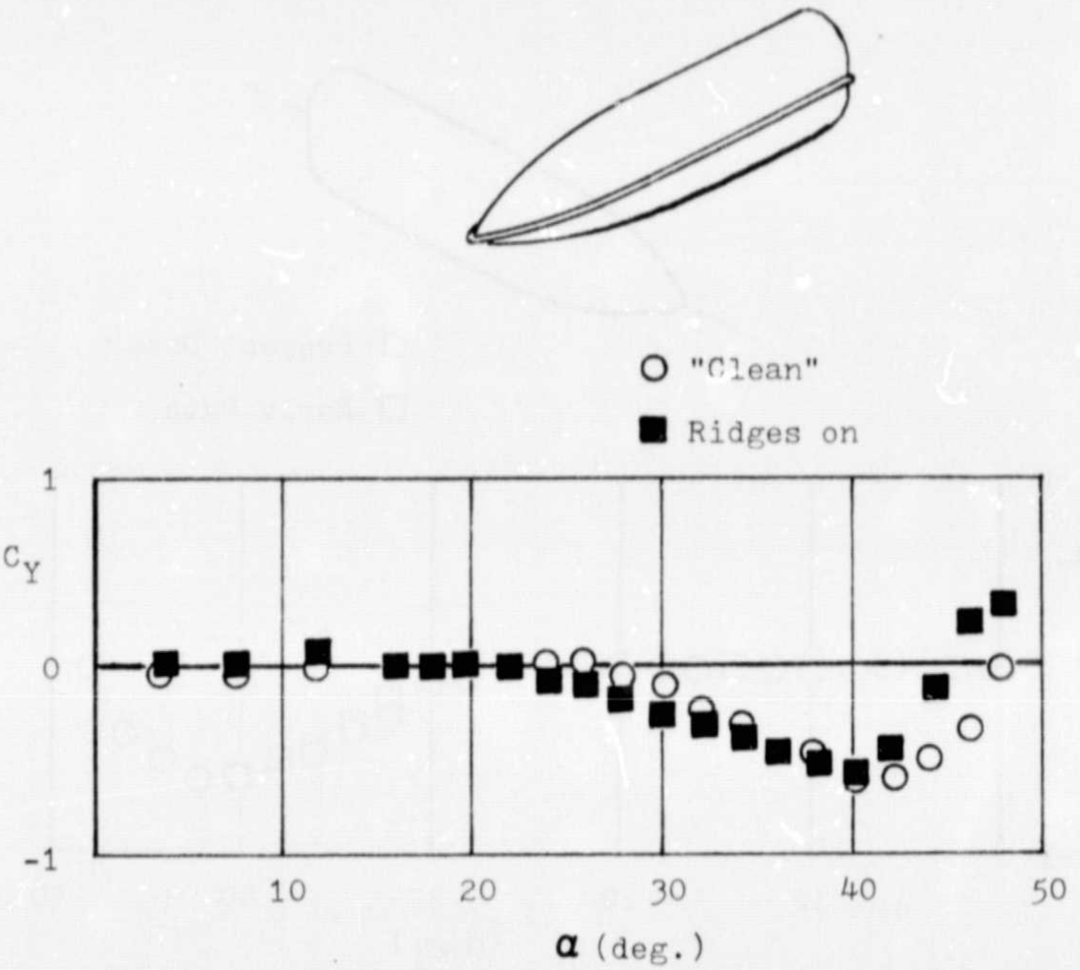

Fig.4 Forebody with 1/8 inch straight ridges (Model I): Side force coeff. versus angle of attack.

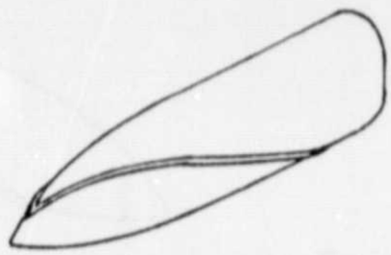

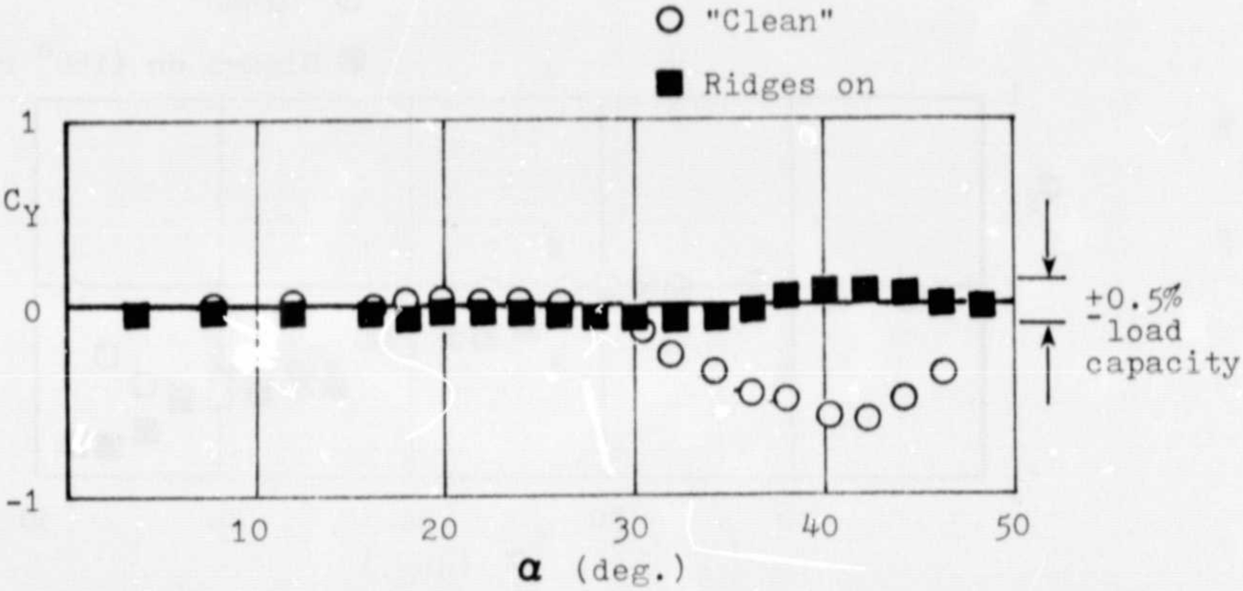

Fig.5 Forebody with 1/8 inch helical ridges (Model I): Side force coeff. versus angle of attack.

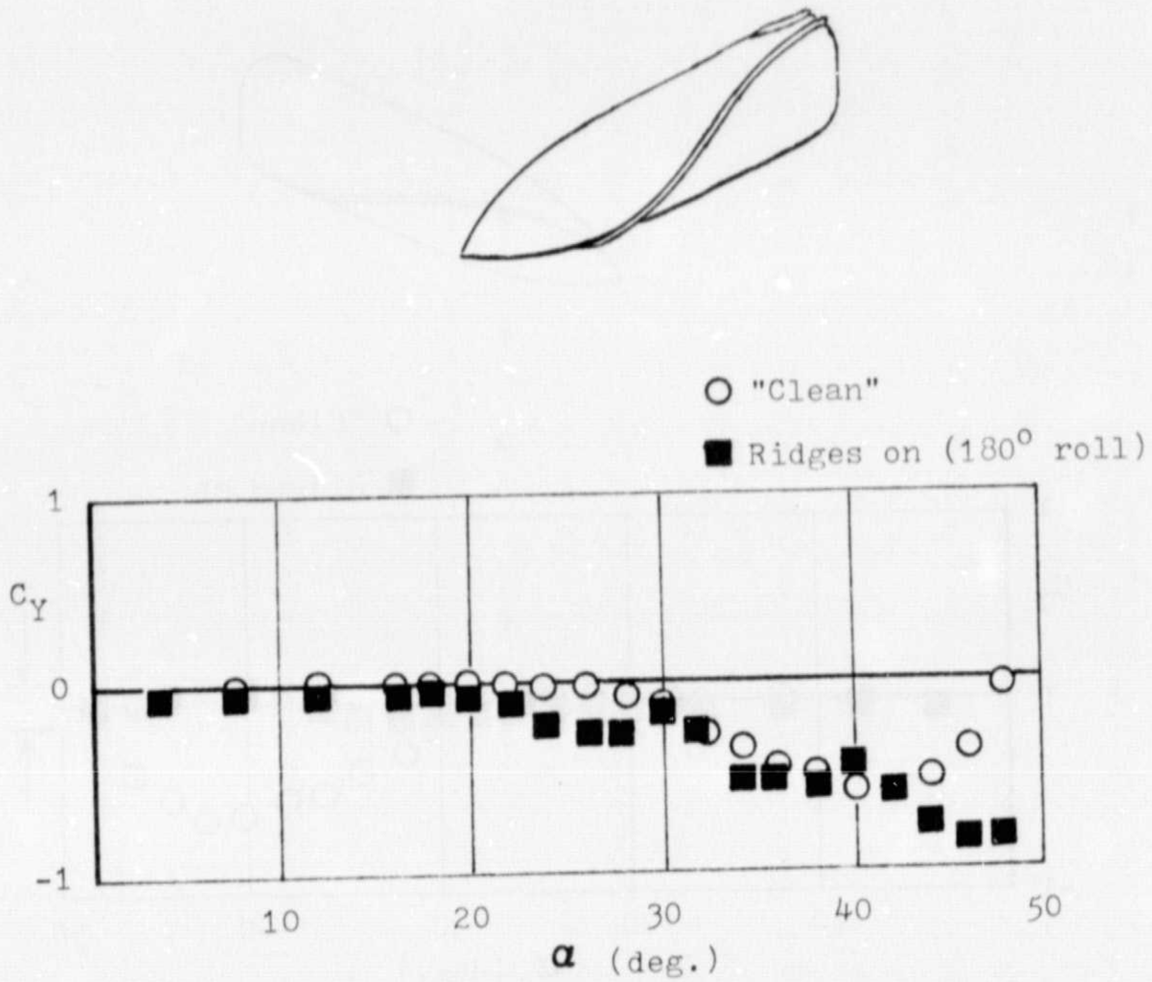

Fig.6 Forebody with 1/8 inch helical ridges (Model I), 180° roll: Side force coeff. versus angle of attack.

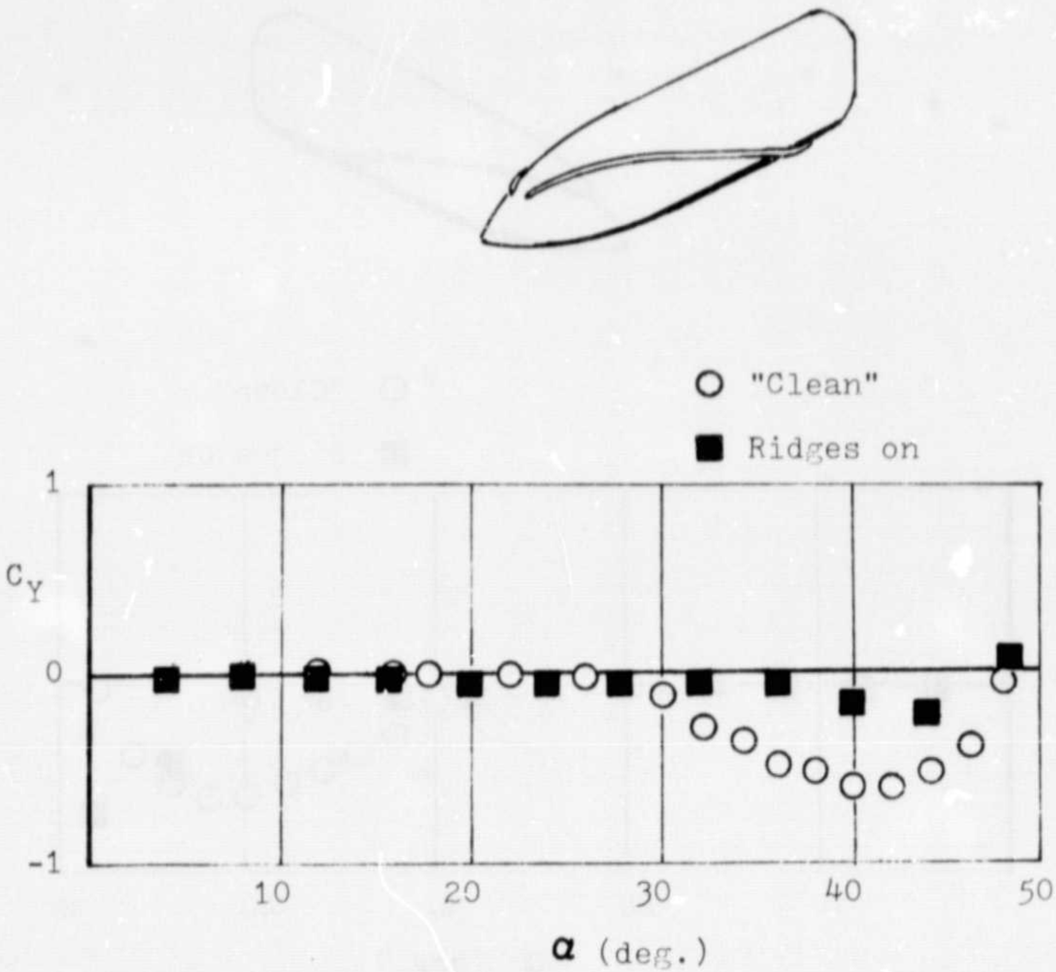

Fig.7 Forebody with 1/8 inch truncated helical ridges, (Model I): Side force coeff. vs. angle of attack.

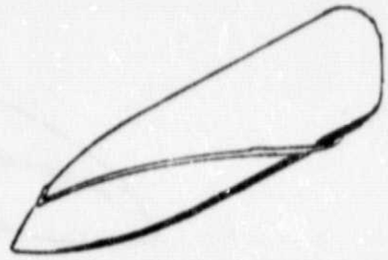

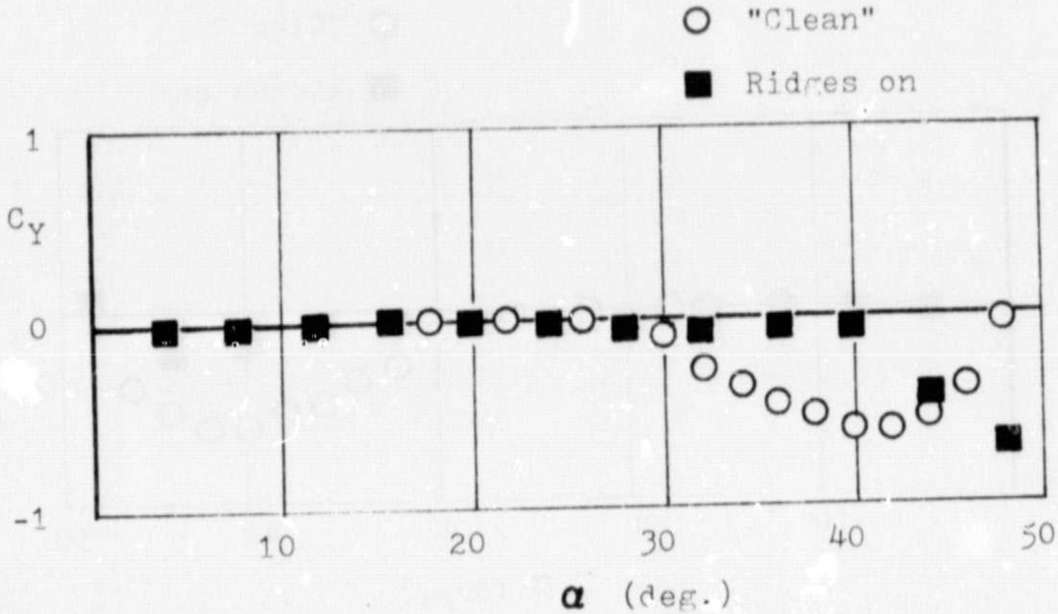

Fig. 8 Forebody with 1/16 inch helical ridges, (Model I): Side force coeff. vs. angle of attack.

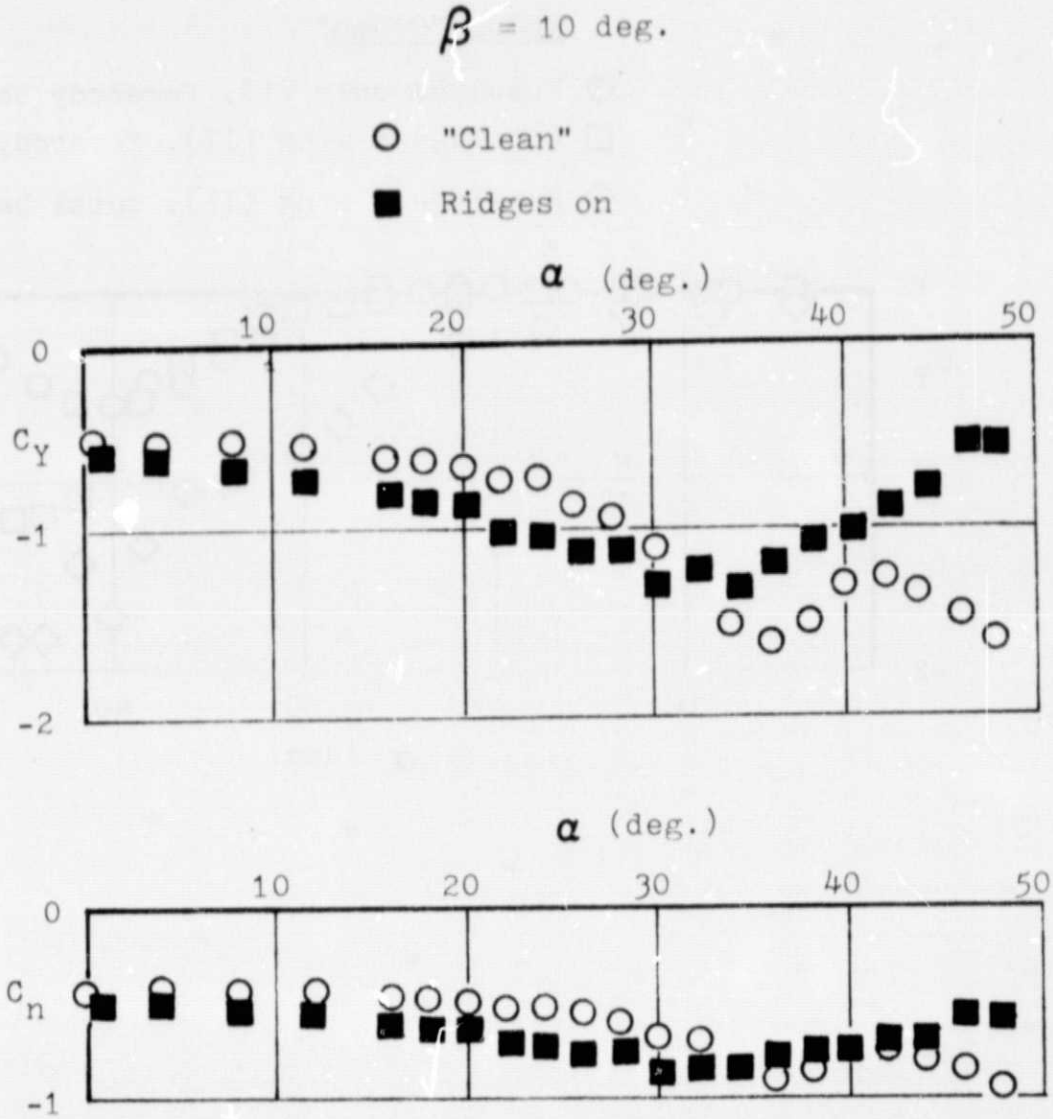

Fig. 9 Forebody with 1/8 inch helical ridges (Model I), 10 deg. sideslip: Side force and Yawing moment coeff. vs. angle of attack.

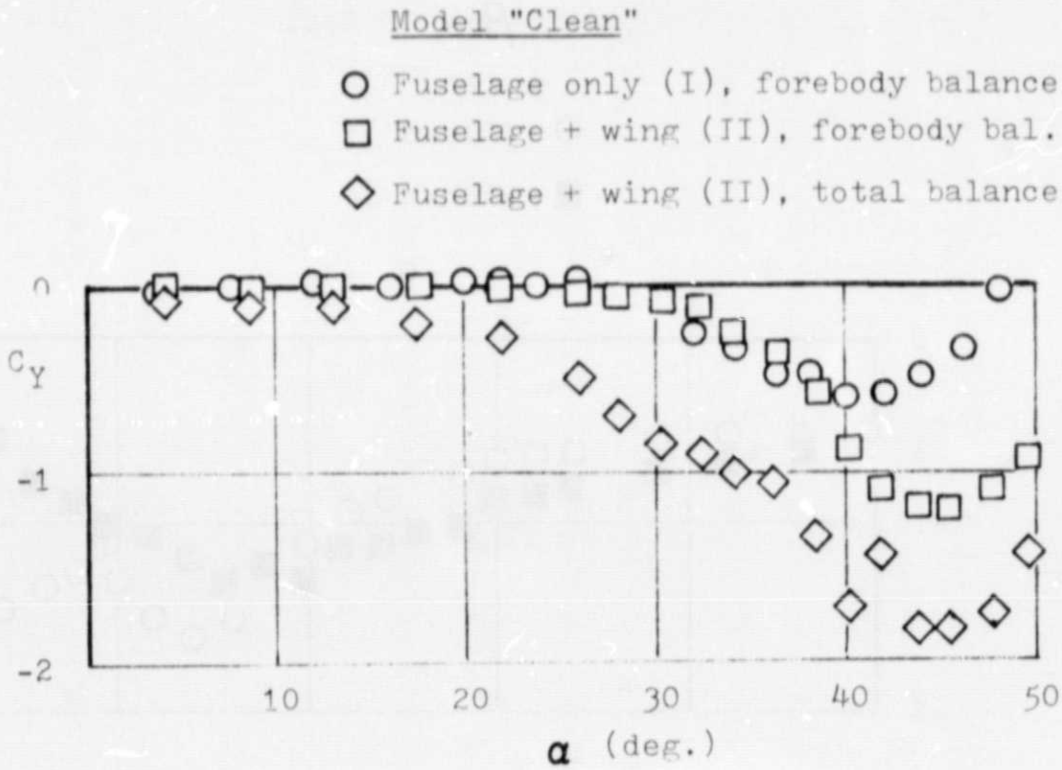

Fig. 10 Comparison of Models I and II with "clean" forebody: Side force coeff. vs. angle of attack.

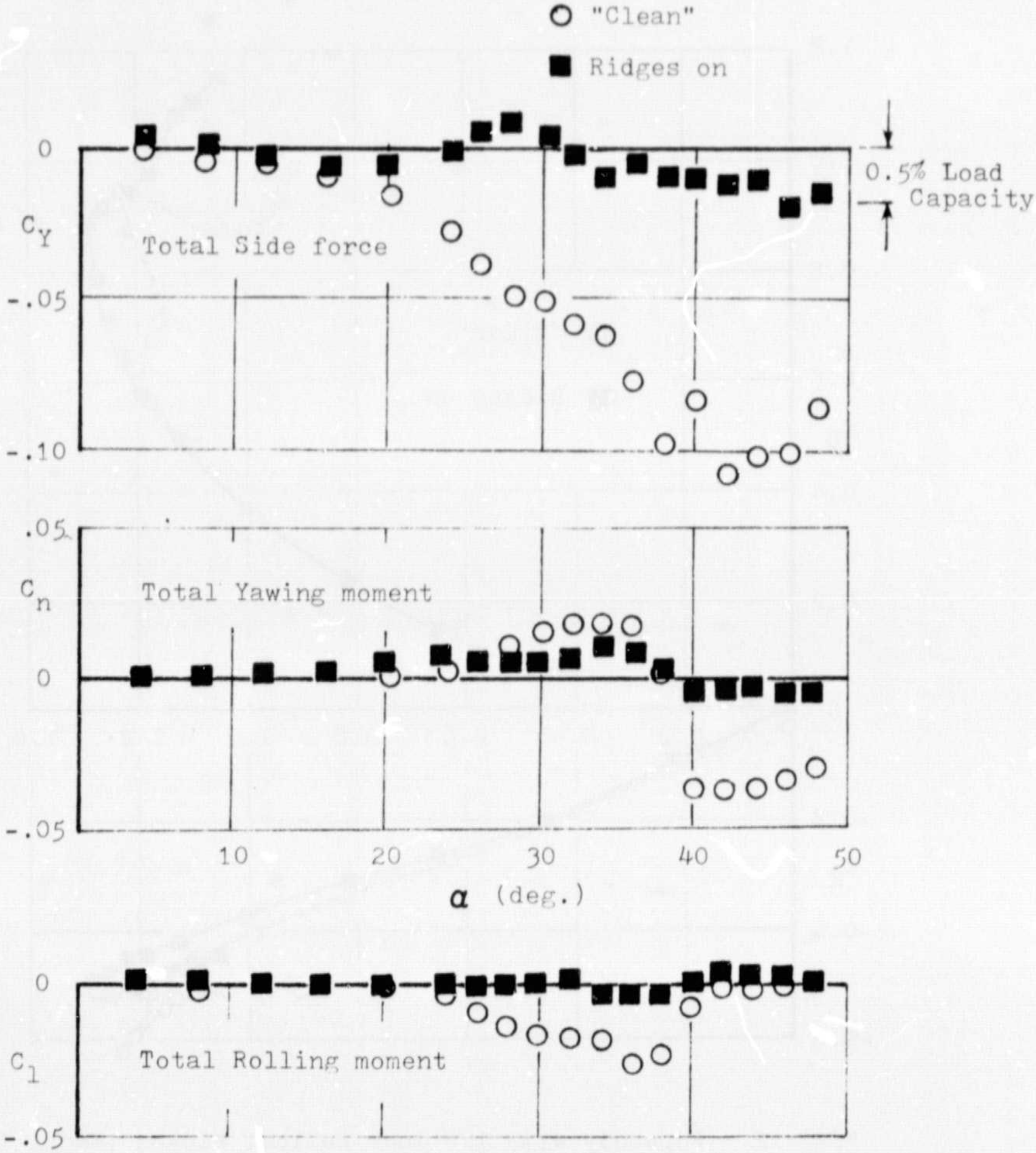

Fig. 11 Forebody with 1/8 inch helical ridges (Model II): Total side force, yawing and rolling moment coeff. vs. angle of attack.

ORIGINAL PAGE IS
OF POOR QUALITY

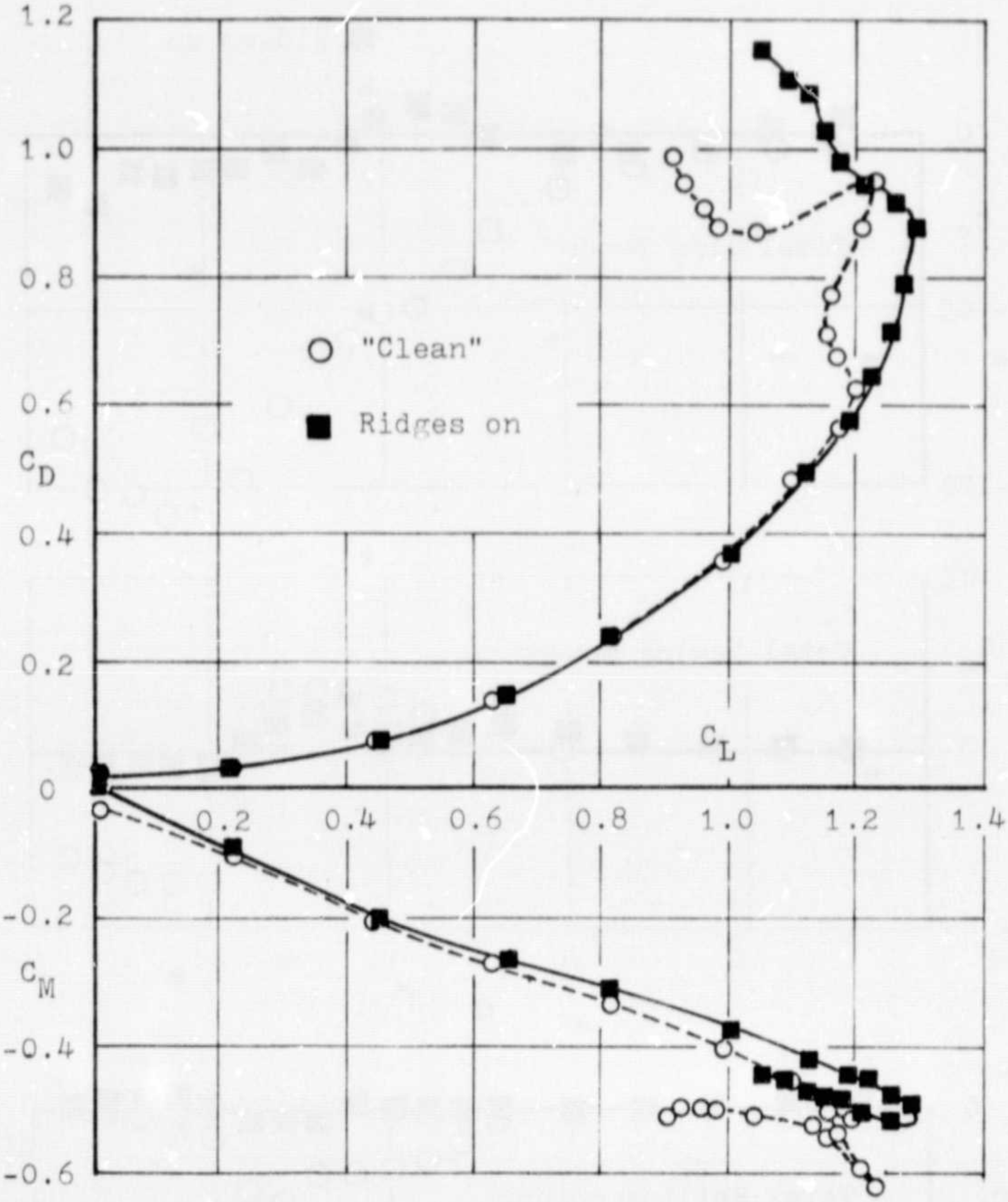

Fig. 12 Forebody with 1/8 inch helical ridges (Model II): Total drag and pitching-moment coeff. vs. angle of attack.

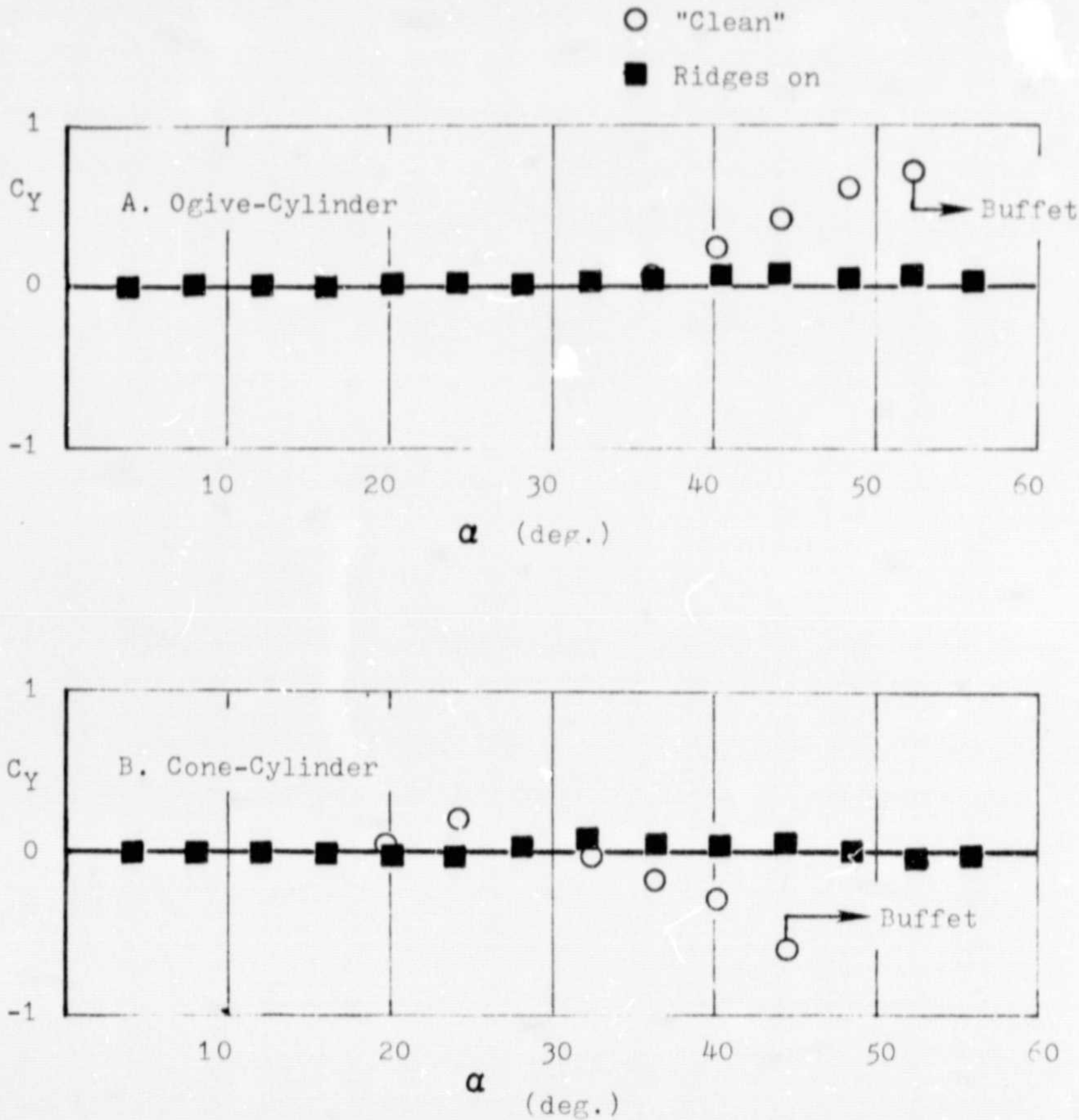

Fig. 13 Forebody with 1/8 inch helical ridges (Models III): Total side force coeff. vs. angle of attack.

1. Report No. NASA CR-145361

2. Government Accession No.

3. Recipient's Catalog No.

4. Title and Subtitle
SIDE-FORCE ALLEVIATION ON SLENDER, POINTED FOREBODIES AT HIGH ANGLES-OF-ATTACK

5. Report Date
May 1978

6. Performing Organization Code
505-11-13-03

7. Author(s)
Dhanvada M. Rao

8. Performing Organization Report No.

10. Work Unit No.

9. Performing Organization Name and Address
Old Dominion University Research Foundation
Norfolk, Virginia

11. Contract or Grant No.
NSG-1315

12. Sponsoring Agency Name and Address
National Aeronautics and Space Administration
Washington, DC 20546

13. Type of Report and Period Covered
Contractor Report

14. Sponsoring Agency Code

15. Supplementary Notes

16. Abstract

A new device* has been proposed for alleviating high angle-of-attack side force on slender, pointed forebodies. A symmetrical pair of separation trips in the form of helical ridges are applied to the forebody to disrupt the primary lee-side vortices and thereby avoid the instability that produces vortex asymmetry. Preliminary wind tunnel tests at Mach 0.3 and Reynolds no. 5.25 x 10^6 on a variety of forebody configurations and on a wing-body combination at angles of attack up to 56 degrees, demonstrated the effectiveness of the device.

*Patent applied for.

17. Key Words (Suggested by Author(s))
Vortices
Wind-tunnel tests
Wing-body configurations

18. Distribution Statement
Unclassified - Unlimited

19. Security Classif. (of this report)	20. Security Classif. (of this page)	21. No. of Pages	22. Price*
Unclassified	Unclassified	23	$4.00

*For sale by the National Technical Information Service, Springfield, Virginia 22161